A 110 W E-scooter Wireless Charger Operating at 6.78 MHz with Ferrite Shielding

Christopher H. Kwan*†, Juan M. Arteaga*†, Nunzio Pucci†, David C. Yates*† and Paul D. Mitcheson*†
*Bumblebee Power Ltd, London, United Kingdom
†Department of Electrical and Electronic Engineering, Imperial College London, London, United Kingdom
christopher.kwan@imperial.ac.uk

***Abstract*—This paper reports on the design, construction and integration of a wireless inductive charging solution for an electric scooter, operating at a frequency of 6.78 MHz and providing an output power of 110 W. With the use of a push-pull Class EF inverter at the transmit end, as well as ferrite shielding and a voltage-doubler full-wave Class D rectifier at the receive end, this system achieved a DC-DC IPT efficiency of 69%–75% and exhibited good tolerance to misalignment at full charging power.**

***Index Terms*—Inductive power transmission, inductive charging, electric vehicles**

I. Introduction

This paper describes the design and construction of a 6.78 MHz ISM-band wireless charging system for an electric scooter, operating at up to 110 W and with good tolerance to misalignment. In recent years, there has been a huge increase in the popularity and uptake of various forms of micro E-mobility including electric bikes and electric scooters. The incorporation of wireless charging to these vehicles can offer enormous benefits in terms of safety, convenience and reliability, in comparison with existing methods of wired charging and battery swapping. Examples given in [1], show the possibility of implementing a wireless power solution onto electric scooters, and the works in [2], [3] have shown that ISM-band wireless charging is feasible for electric mopeds, with up to 600 W of power delivered to the battery.

In this work, the proposed wireless charging system was integrated into a Segway Ninebot-based electric scooter (Fig. 1). The amount of power to be transferred was determined by the specifications of an off-the-shelf battery charger, which can provide up to 84 W (2 A, 42 V) to the battery of the E-scooter. However, the inductive charging link was demonstrated to work up to 110 W with a test load. A transmit pad, positioned 1 cm off the ground, was used to generate the high-frequency magnetic flux. The receive unit was situated under the E-scooter, where there is a reasonably large and flat area (14 cm by 43 cm). While the receiver coil can be made relatively large, it needs to be very thin so as not to excessively reduce the ground clearance of the E-scooter. The low-profile requirement also applies to any electronics that may need to be placed under the E-scooter, e.g. the rectifier. The bottom of the E-scooter consists of solid aluminium alloy plate; therefore, a form of shielding is required to mitigate the effects of eddy currents being induced in the aluminium.

Fig. 1. E-scooter used in this work [6]

These eddy currents can degrade the performance of the link, due to a reduction in the coil Q factor, coupling factor and link efficiency ([4], [5]).

II. Inductive link design

An operating frequency of 6.78 MHz was selected for this system, which is an ISM band. Fig. 2 shows the geometry and dimensions of the designed transmitter and receiver coils. The transmit coil is a two-turn PCB coil with a width of 25 cm, a length of 30 cm, and a trace width of 1 cm. The inductance of the transmit coil, measured with a Keysight E4990A Impedance Analyser and 42941A Impedance Probe, is 2.66 µH. The receiver coil is a three-turn PCB coil with a width of 11.5 cm, a length of 23.5 cm, and a trace width of 0.5 cm. Ferrite sheets were placed behind the receiver coil to shield the high-frequency magnetic field from the E-scooter's aluminium alloy base; the particular type chosen for this application is the Würth Elektronik Flexible Sintered Ferrite Sheet (364003). The inductance of the receive coil in situ is 2.61 µH.

Due to the E-scooter's base not being perfectly parallel with the ground when stationary on its kickstand, the receiver coil is between 65 mm and 80 mm away from the transmit pad, which in itself is raised up from the ground by 1 cm.

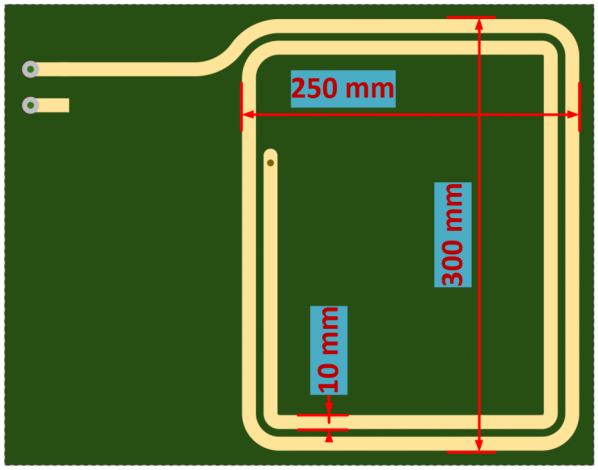

(a) Transmitter coil

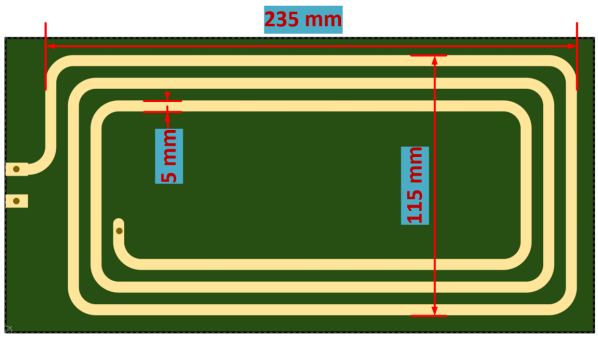

(b) Receiver coil

Fig. 2. PCB coils for E-scooter wireless charger

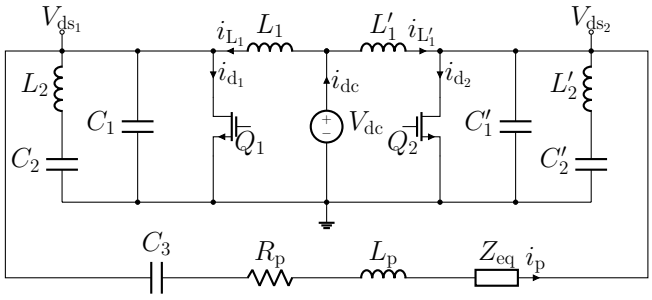

Fig. 3. Circuit diagram of push-pull Class EF inverter

III. High-frequency power electronics

A. Push-pull Class EF inverter

At the transmit side, a push-pull Class EF inverter [7] was used to drive the ground charging pad. The circuit diagram of this class of inverter is shown in Fig. 3, with the component types and implemented values given in Table I. This particular design gives an output current of around 8 A with an input voltage of 67 V.

B. Voltage-doubler full-wave Class D rectifier

A voltage-multiplier full-wave Class D rectifier [8] was integrated into the receive unit which was mounted under the E-scooter's base. Such rectifiers are simple to implement and design. Since the battery charger used in the application has an undervoltage protection, it is important to ensure that the rectifier outputs a voltage that does not trigger the undervoltage protection system throughout the expected range of coupling. Therefore, based on the selection of the coil dimensions and subsequent calculation of the resulting link parameters, a voltage-doubler topology was chosen accordingly, whose circuit diagram is shown in Fig. 4. Table II lists the component values used in the implementation of the rectifier. D_{1-4} are Vishay MBRF10100 Schottky diodes.

TABLE I
Component values and parts used in push-pull Class EF inverter

Parameter	Value/Implementation
C_1, C_1'	731 pF TDK C0G SMD MLCC
C_2, C_2'	704 pF TDK C0G SMD MLCC
C_3	518 pF Vishay QUAD HIFREQ MLCC
L_1	88 µH Coilcraft DO5010H
L_2, L_2'	187 nH Coilcraft 2014VS
L_p	2.61 µH PCB coil
Q_1, Q_2	GaN Systems GS66508B
Gate drivers	TI UCC27512DRSR

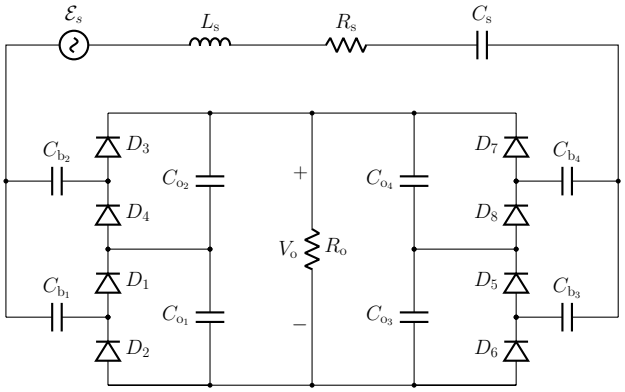

Fig. 4. Circuit diagram of full-wave voltage doubler Class D rectifier

TABLE II
Component values of the voltage-doubler full-wave Class D rectifier

Topology	C_s [pF]	$C_{b_{1-4}}$ [nF]	$C_{o_{1-4}}$ [µF]
2x voltage-multiplier full-wave Class D	223	100	0.3

IV. Experimental results

Fig. 5 shows the experimental setup of the DC-DC IPT system, with the receiver unit mounted under the E-scooter. Table III shows the results of this system running at an output power level of 110 W. Fig. 6 shows the oscilloscope traces of the drain-source voltage of both GaN transistors in the push-pull Class EF inverter; the V_{DS} waveform reached

Fig. 5. DC-DC system experimental setup

TABLE III
DC-DC IPT EXPERIMENTAL RESULTS AT 110 W

Quantity	Value
$V_{\text{DC, in}}$	67.0 V
$P_{\text{DC, in}}$	163.28 W
$V_{\text{DC, out}}$	152 V
$P_{\text{DC, out}}$	112.87 W
$\eta_{\text{DC-DC}}$	69.1 %

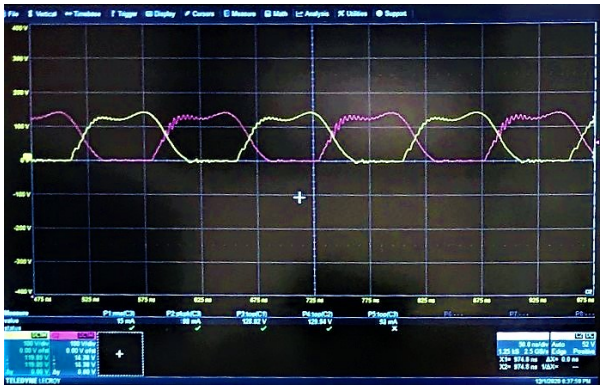

Fig. 6. Oscilloscope traces of V_{DS} of both GaN transistors in push-pull Class EF inverter (Vertical scale is 100 V/div)

a maximum of 130 V. Based on circuits simulations with component values given in Tables I and II and the results in Table III, a coupling factor of 12.2 % was estimated with perfect coil alignment.

After performing the DC-DC IPT experiments, a mains-to-48VDC interface (Mean Well ERPF-400-48), a 48 V to 67 V boost stage (Analog Devices DC2744A evaluation board with LTC8740 boost converter), the off-the-shelf 84 W battery charger and the battery were added to the IPT system. The efficiency of each block in the entire mains-to-battery system was characterised (assuming an output power of 84 W), and is shown in Table IV. At this level of power throughput, the distribution of losses in the entire system is shown in Fig. 7.

TABLE IV
EFFICIENCY OF EACH SYSTEM BLOCK

Block	Efficiency
Mains-to-DC interface (η_{PFC})	87.95 %
Boost stage (η_{boost})	94.3 %
DC-DC IPT ($\eta_{\text{IPT, DC-DC}}$)	69 %–75 %
Battery charger (η_{charger})	90 %
Overall ($\eta_{\text{PFC}} * \eta_{\text{boost}} * \eta_{\text{IPT, DC-DC}} * \eta_{\text{charger}}$)	51 %–56 %

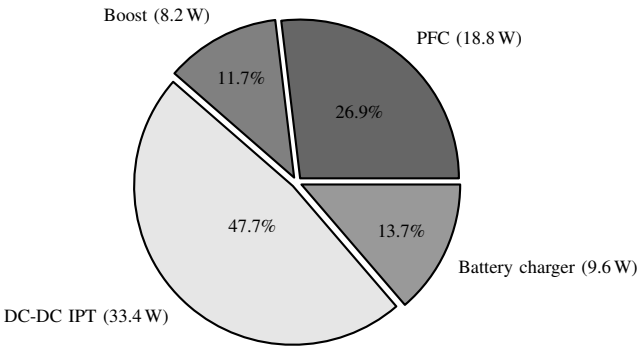

Fig. 7. Distribution of mains-to-load losses with an output power of 84 W

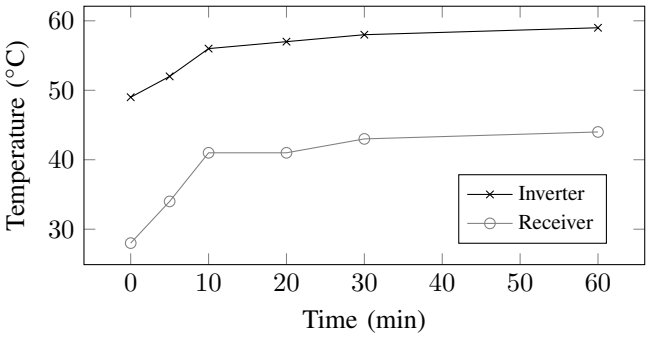

Fig. 8. Evolution of temperature at the transmit and receive ends

A thermal characterisation of the wireless charging system was performed by recording the evolution of temperature whilst running the wireless charger for one hour. Fig. 8 shows the the maximum temperature measured by a thermal camera at the transmit and receive ends. At the transmit end, the highest temperature of 59 °C was measured on the GaN transistor, whilst at the receive end, the maximum temperature of 44 °C occurred on the ferrite sheet.

Fig. 9 illustrates the two methods used to evaluate the performance of the wireless charging system with misalignments between the transmit ground pad and the E-scooter receive unit. The first method was to add angular misalignment by swinging the back wheel to one side whilst keeping the front wheel in a fixed position. It was found that by moving the back wheel to the right by 10 cm, the system remained capable of delivering the full power to the load. The second method involved moving scooter laterally; the system could

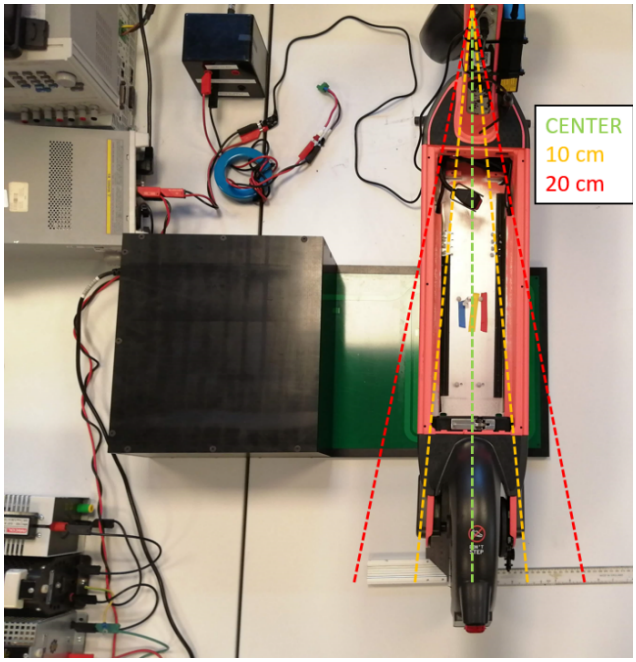

(a) Back wheel angular misalignment

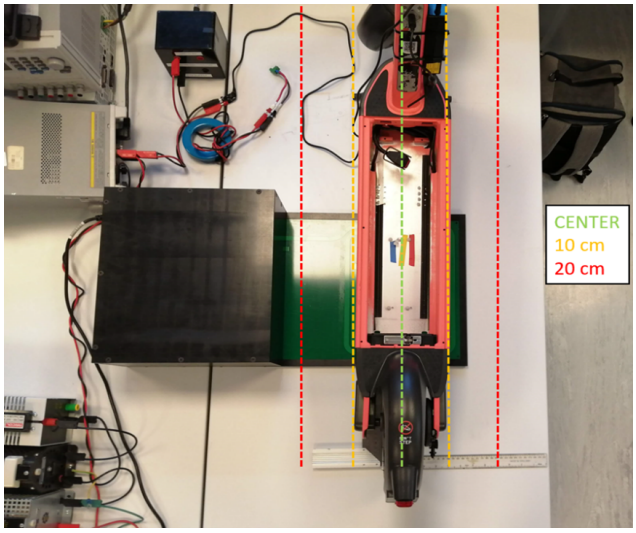

(b) Lateral misalignment

Fig. 9. Setup for E-scooter misalignment testing

still charge the battery at full power after shifting the scooter 7.5 cm to the right.

Increasing the misalignment even more caused the undervoltage protection circuitry of the off-the-shelf battery charger to activate, thus disabling the charger. With greater misalignment, the mutual inductance of the coupled coils decreases further, which means that to receive the same amount of power, more current needs to flow in the receiver (assuming the transmit coil current and output power remain the same). However, a higher current draw can cause the receiver voltage to drop below the undervoltage limit.

V. Conclusion

The primary challenge with integrating a wireless charger into an E-scooter lies in the magnetic link design, which for this particular application has very specific requirements. Some of the constraints include the proximity of the receive unit to the bottom of the E-scooter consisting of a large aluminium alloy plane, the need for the receive unit to be as thin as possible, as well as ensuring good tolerance to coil misalignments. With the use of ferrite shielding at the receiver end, the selection of appropriate coil sizes, and the use of high-frequency resonant power converter topologies, a 6.78 MHz, 110 W wireless charging system with a DC-DC IPT efficiency of 69 %–75 % was successfully developed and implemented into an E-scooter.

Acknowledgement

The authors would like to thank Voi for partnering with Bumblebee Power [9] and providing the E-scooter; and would like to acknowledge the following funding sources: EPSRC Quietening ultra-low-loss SiC & GaN waveforms, grant ref: EP/R029504/1; EPSRC Impact Acceleration Account - Imperial College London 2017, grant ref: EP/R511547/1; EPSRC Converter Architectures, grant ref: EP/R004137/1; SitS NSF-UKRI: Wireless In-Situ Soil Sensing Network for Future Sustainable Agriculture', grant ref: NE/T011467/1; and the Department of Electrical and Electronic Engineering, Imperial College London.

References

[1] J. Hu, F. Lu, C. Zhu, C. Cheng, S. Chen, T. Ren, and C. C. Mi, "Hybrid energy storage system of an electric scooter based on wireless power transfer," *IEEE Transactions on Industrial Informatics*, vol. 14, no. 9, pp. 4169–4178, 2018.

[2] C. H. Kwan, J. M. Arteaga, D. C. Yates, and P. D. Mitcheson, "Design and construction of a 100 w wireless charger for an e-scooter at 6.78 mhz," in *2019 IEEE PELS Workshop on Emerging Technologies: Wireless Power Transfer (WoW)*, 2019, pp. 186–190.

[3] C. H. Kwan, J. M. Arteaga, S. Aldhaher, D. C. Yates, and P. D. Mitcheson, "A 600w 6.78mhz wireless charger for an electric scooter," in *2020 IEEE PELS Workshop on Emerging Technologies: Wireless Power Transfer (WoW)*, 2020, pp. 278–282.

[4] C. H. Kwan, G. Kkelis, S. Aldhaher, J. Lawson, D. C. Yates, P. C. . Luk, and P. D. Mitcheson, "Link efficiency-led design of mid-range inductive power transfer systems," in *2015 IEEE PELS Workshop on Emerging Technologies: Wireless Power (2015 WoW)*, 2015, pp. 1–7.

[5] M. Pinuela, D. C. Yates, S. Lucyszyn, and P. D. Mitcheson, "Maximizing dc-to-load efficiency for inductive power transfer," *IEEE Transactions on Power Electronics*, vol. 28, no. 5, pp. 2437–2447, 2013.

[6] "Voi Vehicles - Our Voi scooters and bikes," https://www.voiscooters.com/voi-vehicles/, January 2021.

[7] S. Aldhaher and P. D. Mitcheson, "500w 13.56mhz class ef push-pull inverter for advanced dynamic wireless power applications," in *2019 IEEE PELS Workshop on Emerging Technologies: Wireless Power Transfer (WoW)*, 2019, pp. 263–267.

[8] M. M. Weiner, "Analysis of cockcroft-walton voltage multipliers with an arbitrary number of stages," *Review of Scientific Instruments*, vol. 40, no. 2, pp. 330–333, 1969.

[9] Voi. Voi partners with imperial college spin-out bumblebee power to enable wireless charging of micro-mobility vehicles. [Online]. Available: https://www.voiscooters.com/blog/voi-partners-with-imperial-college-spin-out-bumblebee-power/